Doppler Synthetic Aperture Hitchhiker Imaging

Can Evren Yarman
Houston Technology Center
WesternGeco, Schlumberger
Houston, TX 77042

Birsen Yazıcı
Department of Electrical, Computer
and System Engineering
Rensselaer Polytechnic Institute
Troy, New York 12180–3590
Email: yazici@ecse.rpi.edu

Abstract— **In this paper we consider passive airborne receivers that use backscattered signals from sources of opportunity that transmit fixed-frequency waveforms to form an image of the ground. Due to its combined passive synthetic aperture and fixed-frequency nature of the transmitted waveforms, we refer to the system under consideration as Doppler Synthetic Aperture Hitchhiker (DSAH). We present a novel image formation method for DSAH. Our method first correlates the windowed signal obtained from one receiver with the scaled and transmitted version of the received signal from another receiver and then forms the image of the scene radiance by weighted-backprojection of the correlated signal. The method is applicable with both cooperative and non-cooperative sources of opportunity, mobile and stationary sources and one or more receivers. Additionally, it is an analytic reconstruction technique which can be made computationally efficient.**

I. Introduction

In recent years, there has been a renewed and growing interest in passive radar applications using sources of opportunity [1], [2], [3]. This research effort is motivated by growing availability of transmitters of opportunity, such as radio, television and cell phone stations, particularly in urban areas, as well as relatively low cost and rapid deployment of passive receivers.

While many of passive radar applications are focused on detection of airborne targets with ground based receivers [4], [5], [1], [2], [3], recently, there has been research effort in developing synthetic aperture passive imaging methods using airborne receivers [6], [7], [8]. In [7], [8], we reported a novel passive synthetic aperture imaging method that is based on spatio-temporal correlation of the data and generalized filtered-backprojection techniques. While this method is applicable to any transmit waveform in principle, the data collection manifold for the case of single frequency transmitters is limited. In urban areas, however, most of the transmitters of opportunity are single frequency sources, such as FM radio stations. In this paper, we develop a new passive synthetic aperture image formation method for sources that transmit fixed-frequency waveforms. These waveforms are also referred to as high-Doppler-resolution or continuous wave (CW) waveforms. Thus, we refer to the resulting method as Doppler synthetic aperture hitchhiker imaging method.

In our current discussion, for simplicity, we consider a single, static transmitter with known location and two SAR receivers traversing arbitrary, but known, flight trajectories as shown in Figure 1. Our method first correlates the windowed signal obtained from one receiver with the scaled and transmitted version of the received signal from the other receiver, and then forms the image of the scene radiance by weighted-backprojection of the correlated signal.

Our method can be characterized as a microlocal technique that combines synthetic aperture hitchhiker imaging method that we introduced in [7], [8] with the monostatic Doppler SAR imaging method of [9]. Our method has the following practical advantages: (1) as compared to the existing passive radar detection systems [10], [11], [12], [13], [14], [15], [16], [2], it does not require receivers with high directivity; (2) it can be used in the presence of both cooperative and non-cooperative sources of opportunity; (3) it can be used with stationary and/or mobile sources of opportunity; (4) it can be used with one or more airborne receivers. However, to keep our discussion focused, we introduce our imaging method for a single cooperative transmitter and two airborne antennas.

The organization of the paper is as follows. In Section II, we introduce the bistatic SAR data model. In Section III, we present the correlated measurements and the resulting model between the correlated measurements and ground radiance. In Section IV, we develop the weighted-backprojection type image formation process. Finally, we conclude our discussion in Section V.

1-4244-1539-X/08/$25.00 ©2008 IEEE

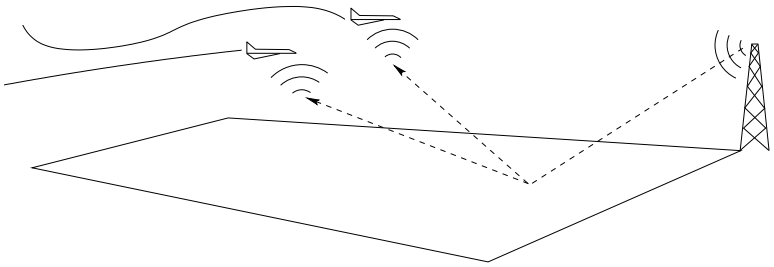

Fig. 1. Passive synthetic aperture radar Doppler imaging geometry.

II. Measurement Model

Given a pair of transmitter and receiver antennas located at $\mathbf{T}$ and $\mathbf{R}$ respectively, we model the received signal by [17]

$$f(t,\mathbf{R},\mathbf{T}) \approx \int \frac{\mathrm{e}^{-\mathrm{i}\omega(t-(|\mathbf{R}-\mathbf{z}|+|\mathbf{z}-\mathbf{T}|)/c_0)}}{(4\pi)^2|\mathbf{R}-\mathbf{z}||\mathbf{z}-\mathbf{T}|}\omega^2 \times J_{\mathrm{tr}}(\omega,\widehat{\mathbf{z}-\mathbf{T}},\mathbf{T})J_{\mathrm{rc}}(\omega,\widehat{\mathbf{z}-\mathbf{R}},\mathbf{R})V(\mathbf{z})d\omega\,d\mathbf{z}, \quad (1)$$

where $V(\mathbf{z})$ is the reflectivity function; and J_{tr} and J_{rc} are the transmitter and receiver antenna beam patterns.

For a fixed-frequency waveform with frequency ω_0, the received signal becomes [9]

$$f(t,\mathbf{R},\mathbf{T}) \approx \int \frac{\mathrm{e}^{-\mathrm{i}\omega_0(t-(|\mathbf{R}-\mathbf{z}|+|\mathbf{z}-\mathbf{T}|)/c_0)}}{(4\pi)^2|\mathbf{R}-\mathbf{z}||\mathbf{z}-\mathbf{T}|}\omega_0^2 \times J_{\mathrm{tr}}(\omega_0,\widehat{\mathbf{z}-\mathbf{T}},\mathbf{T})J_{\mathrm{rc}}(\omega_0,\widehat{\mathbf{z}-\mathbf{R}},\mathbf{R})V(\mathbf{z})\,d\mathbf{z}, \quad (2)$$

where $\widehat{\mathbf{x}} = \mathbf{x}/|\mathbf{x}|$ denotes the unit vector in the direction of $\mathbf{x}$.

Without loss of generality, for the rest of the paper, we assume that the transmitter is stationary at location $\mathbf{T}$ and that two airborne receivers are traversing the trajectories $\boldsymbol{\gamma}_1(t)$ and $\boldsymbol{\gamma}_2(t)$. We define

$$s_i(t) = f(t,\boldsymbol{\gamma}_i(t),\mathbf{T}), \quad i=1,2 \quad (3)$$

to be the signal received at time t by the receiver i.

III. Correlation of Measurements

We define the correlation of the received signals s_1 and s_2 by

$$c_{12}(\tau_1,\tau_2,\mu) = \int s_1(t+\tau_1)s_2^*(\mu t+\tau_2)\phi(t)\,dt, \quad (4)$$

where * denotes complex conjugation and $\phi(t)$ is a smooth compactly supported time windowing function centered at $t=0$; in other words, c_{12} is the windowed cross correlation of s_1 and s_2.

Substituting s_i, $i=1,2$ into c_{12}, we obtain

$$c_{12}(\tau_1,\tau_2,\mu) = \frac{\omega_0^4}{(4\pi)^4}\int \mathrm{e}^{-\mathrm{i}\omega_0(t+\tau_1-(|\boldsymbol{\gamma}_1(t+\tau_1)-\mathbf{z}|+|\mathbf{T}-\mathbf{z}|)/c_0)} \times \mathrm{e}^{\mathrm{i}\omega_0(\mu t+\tau_2-(|\boldsymbol{\gamma}_2(\mu t+\tau_2)-\mathbf{z}'|+|\mathbf{T}-\mathbf{z}'|)/c_0)} \times \frac{W_1(t+\tau_1,\mathbf{z})W_2^*(\mu t+\tau_2,\mathbf{z}')}{G_{12}(t,\mathbf{z},\tau_1,\tau_2,\mu)} \times V(\mathbf{z})V^*(\mathbf{z}')d\mathbf{z}\,d\mathbf{z}'\phi(t)\,dt, \quad (5)$$

where G_{12} is the product of the geometric spreading factors,

$$G_{12}(\mathbf{z},t,\tau_1,\tau_2,\mu) = |\mathbf{T}-\mathbf{z}|\,|\mathbf{T}-\mathbf{z}'| \times |\boldsymbol{\gamma}_1(t+\tau_1)-\mathbf{z}|\,|\boldsymbol{\gamma}_2(\mu t+\tau_2)-\mathbf{z}'|, \quad (6)$$

and

$$W_i(t,\mathbf{z}) = J_{\mathrm{tr}}(\omega_0,\widehat{\mathbf{z}-\mathbf{T}},\mathbf{T}) \times J_{\mathrm{rc}}(\omega_0,\widehat{\mathbf{z}-\boldsymbol{\gamma}_i(t)},\boldsymbol{\gamma}_i(t)), \quad i=1,2, \quad (7)$$

is the product of the transmitter and receiver antenna beam patterns.

We make the assumptions that the earth's surface is located at the position given by $\mathbf{z} = \boldsymbol{\psi}(\boldsymbol{z})$, where now $\boldsymbol{z}\in\mathbb{R}^2$ and $\boldsymbol{\psi}:\mathbb{R}^2\longrightarrow\mathbb{R}^3$ is known; and the scattering takes place in a thin region near the surface and the reflectivity function is in the form

$$V(\mathbf{z}) = \rho(\boldsymbol{z})\delta(\mathbf{z}-\boldsymbol{\psi}(\boldsymbol{z})). \quad (8)$$

Thus

$$c_{12}(\tau_1,\tau_2,\mu) = \frac{\omega_0^4}{(4\pi)^4}\int \mathrm{e}^{-\mathrm{i}\omega_0(t+\tau_1-(|\boldsymbol{\gamma}_1(t+\tau_1)-\mathbf{z}|+|\mathbf{T}-\mathbf{z}|)/c_0)} \times \mathrm{e}^{\mathrm{i}\omega_0(\mu t+\tau_2-(|\boldsymbol{\gamma}_2(\mu t+\tau_2)-\mathbf{z}'|+|\mathbf{T}-\mathbf{z}'|)/c_0)} \times \frac{W_1(t+\tau_1,\mathbf{z})W_2^*(\mu t+\tau_2,\mathbf{z}')}{G_{12}(\mathbf{z},t,\tau_1,\tau_2,\mu)} \times \rho(\boldsymbol{z})\rho^*(\boldsymbol{z}')d\boldsymbol{z}\,d\boldsymbol{z}'\phi(t)\,dt. \quad (9)$$

where ρ is referred to as the ground reflectivity function, and $\mathbf{z}$ should be uderstood as $\psi(\boldsymbol{z})$.

Now using the Taylor series expansion at $t = 0$

$$\boldsymbol{\gamma}_1(t+\tau_1) = \boldsymbol{\gamma}_1(\tau_1) + \dot{\boldsymbol{\gamma}}_1(\tau)t + \dots \tag{10}$$

$$\boldsymbol{\gamma}_2(\mu t+\tau 2) = \boldsymbol{\gamma}_2(\tau_2) + \dot{\boldsymbol{\gamma}}_2(\tau_2)\mu t + \dots, \tag{11}$$

we make the approximations

$$\begin{aligned}|\boldsymbol{\gamma}_1(t+\tau_1) - \mathbf{z}| &\approx |\boldsymbol{\gamma}_1(\tau_1) - \mathbf{z} + \dot{\boldsymbol{\gamma}}_1(\tau)t| \\ &\approx |\boldsymbol{\gamma}_1(\tau_1) - \mathbf{z}| + (\widehat{\boldsymbol{\gamma}_1(\tau_1) - \mathbf{z}}) \cdot \dot{\boldsymbol{\gamma}}_1(\tau_1)t, \end{aligned} \tag{12}$$

and

$$\begin{aligned}|\boldsymbol{\gamma}_2(\mu t+\tau_2) - \mathbf{z}| &\approx |\boldsymbol{\gamma}_2(\tau_2) - \mathbf{z} + \dot{\boldsymbol{\gamma}}_2(\tau)\mu t| \\ &\approx |\boldsymbol{\gamma}_2(\tau_2) - \mathbf{z}| + (\widehat{\boldsymbol{\gamma}_2(\tau_2) - \mathbf{z}}) \cdot \dot{\boldsymbol{\gamma}}_2(\tau_2)\mu t. \end{aligned} \tag{13}$$

Let C_ρ denote the correlation functions of ρ:

$$C_\rho(\boldsymbol{z}, \boldsymbol{z}') = E[\rho(\boldsymbol{z})\rho^*(\boldsymbol{z}')]. \tag{14}$$

Next, we make the incoherent-field approximation [18] by assuming that ρ satisfies the following equality:

$$C_\rho(\boldsymbol{z}, \boldsymbol{z}') = R_\rho(\boldsymbol{z})\delta(\boldsymbol{z} - \boldsymbol{z}'). \tag{15}$$

Note that R_ρ is the average power of electromagnetic radiation emitted by the scene at location $\mathbf{z}$. In this regard, here R_ρ is referred to as the scene radiance [18].

Substituting the approximations (12) and (13), under the assumption (15), we write the expectation of the correlated signal as

$$\begin{aligned}E[c_{12}(\tau_1, \tau_2, \mu)] &\approx \mathcal{F}[R_\rho](\tau_1, \tau_2, \mu) \\ &= \int \mathrm{e}^{-\mathrm{i}\varphi(t, \boldsymbol{z}, \tau_1, \tau_2, \mu)} A_{12}(\boldsymbol{z}, t, \tau_1, \tau_2, \mu) R_\rho(\boldsymbol{z}) d\boldsymbol{z}\, dt, \end{aligned} \tag{16}$$

where

$$\begin{aligned}\varphi(t, \boldsymbol{z}, \tau_1, \tau_2, \mu) = \omega_0 t(1 - \mu + \big[(\widehat{\boldsymbol{\gamma}_1(\tau_1) - \mathbf{z}}) \cdot \dot{\boldsymbol{\gamma}}_1(\tau_1) \\ - \mu(\widehat{\boldsymbol{\gamma}_2(\tau_2) - \mathbf{z}}) \cdot \dot{\boldsymbol{\gamma}}_2(\tau_2)\big]/c_0), \end{aligned} \tag{17}$$

and

$$\begin{aligned}A_{12}(\boldsymbol{z}, t, \tau_1, \tau_2, \mu) &= \frac{W_1(t+\tau_1, \mathbf{z}) W_2^*(\mu t + \tau_2, \mathbf{z})}{G_{12}(\mathbf{z}, t, \tau_1, \tau_2, \mu)} \\ &\times \frac{\omega_0^4\, \phi(t)}{(4\pi)^4} \mathrm{e}^{-\mathrm{i}\omega_0(\tau_1 - \tau_2 - (|\boldsymbol{\gamma}_1(\tau_1) - \mathbf{z}| - |\boldsymbol{\gamma}_2(\tau_2) - \mathbf{z}|)/c_0)}, \end{aligned} \tag{18}$$

We refer to φ and A_{12} as the phase and amplitude functions of the linear operator $\mathcal{F}$, respectively. Note that the correlation of received signals removes all transmitter related terms from the phase of the operator $\mathcal{F}$.

We assume that for some m_A, A_{12} satisfies the following inequality:

$$\begin{aligned}\sup_{(\mu, t, \tau_1, \tau_2, \boldsymbol{z}) \in \mathcal{U}} \left| \partial_t^{\alpha_t} \partial_\mu^{\alpha_\mu} \partial_{\tau_1}^{\beta_1} \partial_{\tau_2}^{\beta_2} \partial_{z_1}^{\epsilon_1} \partial_{z_2}^{\epsilon_2} A_{12}(\boldsymbol{z}, t, \tau_1, \tau_2, \mu) \right| \\ \leq C_A (1 + t^2)^{(m_A - |\alpha_t|)/2} \end{aligned} \tag{19}$$

where $\mathcal{U}$ is any compact subset of $\mathbb{R}^+ \times \mathbb{R}^+ \times \mathbb{R} \times \mathbb{R} \times \mathbb{R}^2$, and the constant C_A depends on $\mathcal{U}, \alpha_{t,\mu}, \beta_{1,2}$ and $\epsilon_{1,2}$. This assumption is needed in order to make various stationary phase calculations hold. In practice (19) is satisfied for transmitters and receivers sufficiently away from the illuminated region. This is the case especially for air-borne transmitters and receivers, and broadcasting stations located on high grounds.

Under the assumption (19), equation (16) defines $\mathcal{F}$ as a *Fourier integral operator* [19] whose leading-order contribution comes from those points satisfying

$$\begin{aligned}(\widehat{\boldsymbol{\gamma}_1(\tau_1) - \mathbf{z}}) \cdot \dot{\boldsymbol{\gamma}}_1(\tau_1) - \mu(\widehat{\boldsymbol{\gamma}_2(\tau_2) - \mathbf{z}}) \cdot \dot{\boldsymbol{\gamma}}_2(\tau_2) \\ = (\mu - 1)c_0 \end{aligned} \tag{20}$$

The first term above is the radial speed of receiver 1 with respect to $\mathbf{z}$, and the second term is the radial speed of receiver 2 with respect to $\mathbf{z}$ scaled by μ.

Let v_1 be the radial velocity of receiver 1 with respect to $\mathbf{z}$. Then, by (20), $\mathcal{F}$ projects the scene radiance function onto the curves $\Gamma_{1,2}(\tau_1, \tau_2, \mu)$ formed by the intersection of the constant-Doppler cones

$$(\widehat{\boldsymbol{\gamma}_1(\tau_1) - \mathbf{z}}) \cdot \dot{\boldsymbol{\gamma}}_1(\tau_1) = v_1 \tag{21}$$

and

$$(\widehat{\boldsymbol{\gamma}_2(\tau_2) - \mathbf{z}}) \cdot \dot{\boldsymbol{\gamma}}_2(\tau_2) = v_2, \tag{22}$$

and earth's surface, where $v_1 \in \mathbb{R}$, $v_2 = [v_1 + (1 - \mu)c_0] / \mu$.

When earth's surface is flat and receiver trajectories are at fixed altitudes, (21) and (22) define two hyperbolas (see Appendix), which we will denote by $H_{1,\tau_1,\tau_2}(v_1)$ and $H_{2,\tau_1,\tau_2,\mu}(v_1)$, respectively. Thus $\mathcal{F}$ projects the scene radiance function onto the curve $\Gamma_{1,2}(\tau_1, \tau_2, \mu)$ which is parameterized by v_1 and defined by the points in the intersection of $H_{1,\tau_1,\tau_2}(v_1)$ and $H_{2,\tau_1,\tau_2,\mu}(v_1)$:

$$\begin{aligned}&\Gamma_{1,2}(\tau_1, \tau_2, \mu) \\ &= \left\{ \boldsymbol{z} \in \mathbb{R}^2 \,\middle|\, \boldsymbol{z} \in \bigcup_{v_1 \in \mathbb{R}} \left[H_{1,\tau_1,\tau_2}(v_1) \bigcap H_{2,\tau_1,\tau_2,\mu}(v_1) \right] \right\}. \end{aligned} \tag{23}$$

Since $\mathcal{F}$ is a Fourier integral operator, we form the image of the scene radiance by a suitable backprojection onto $\Gamma_{1,2}(\tau_1, \tau_2, \mu)$ [19].

IV. Image Formation

From the expected correlation of the measurements (16), we form our image by the weighted-backprojection operation:

$$\begin{aligned}\widetilde{R}_\rho(\boldsymbol{z}) &= \mathcal{K}[\mathcal{F}[R_\rho]](\boldsymbol{z}) \\ &= \int \left[\int \mathrm{e}^{\mathrm{i}\varphi(t,\boldsymbol{z},\tau_1,\tau_2,\mu)} Q_{12}(\boldsymbol{z},t,\tau_1,\tau_2,\mu) dt \right] \\ &\qquad \times E[c_{12}](\tau_1,\tau_2,\mu)\, d\tau_1\, d\tau_2\, d\mu, \quad (24)\end{aligned}$$

where Q_{12} is referred to as weighting function which is to be determined below. We should note that for some m_Q, Q_{12} must satisfy

$$\begin{aligned}\sup_{(\mu,t,\tau_1,\tau_2,\boldsymbol{z})\in\mathcal{U}} &\left| \partial_t^{\alpha_t} \partial_\mu^{\alpha_\mu} \partial_{\tau_1}^{\beta_1} \partial_{\tau_2}^{\beta_2} \partial_{z_1}^{\epsilon_1} \partial_{z_2}^{\epsilon_2} Q_{12}(\boldsymbol{z},t,\tau_1,\tau_2,\mu) \right| \\ &\leq C_Q (1+t^2)^{(m_Q - |\alpha_t|)/2}, \quad (25)\end{aligned}$$

where $\mathcal{U}$ is any compact subset of $\mathbb{R}^+ \times \mathbb{R}^+ \times \mathbb{R} \times \mathbb{R} \times \mathbb{R}^2$, and the constant C_Q depends on $\mathcal{U}, \alpha_{t,\mu}, \beta_{1,2}$ and $\epsilon_{1,2}$. Furthermore, we assume that the amplitude term of the composite operator $\mathcal{KF}$ satisfies a condition similar to (25) so that $\mathcal{KF}$ is a proper Fourier integral operator.

Note that the irrespective of the choice of the weighting function, the backprojection operator recovers the visible edges of the scene radiance at the right location.

Let us rewrite $\widetilde{R}_\rho$ as

$$\widetilde{R}_\rho(\boldsymbol{z}) = \int K(\boldsymbol{z},\boldsymbol{z}') R_\rho(\boldsymbol{z}')\, d\mathbf{z}', \quad (26)$$

where $K(\boldsymbol{z},\boldsymbol{z}')$ is defined as the point spread function of the imaging operator $\mathcal{K}$ given by

$$\begin{aligned}K(\boldsymbol{z},\boldsymbol{z}') = \int &\mathrm{e}^{\mathrm{i}[\varphi(t,\boldsymbol{z},\tau_1,\tau_2,\mu) - \varphi(t',\boldsymbol{z}',\tau_1,\tau_2,\mu)]} \\ &\times Q_{12}(\boldsymbol{z},t,\tau_1,\tau_2,\mu) A_{12}(\boldsymbol{z}',t',\tau_1,\tau_2,\mu) \\ &\times\ dt'\, dt\, d\tau_1\, d\tau_2\, d\mu. \quad (27)\end{aligned}$$

We chose Q_{12} such that the leading order term of the point spread function is Dirac delta function, i.e. $K(\boldsymbol{z},\boldsymbol{z}') \approx \delta(\boldsymbol{z}-\boldsymbol{z}')$.

We use the stationary phase theorem to approximate the t' and μ integrations. We define $\Phi_K = \varphi(t,\boldsymbol{z},\tau_1,\tau_2,\mu) - \varphi(t',\boldsymbol{z}',\tau_1,\tau_2,\mu)$ as the phase of (27) and compute

$$\begin{aligned}\partial_t \Phi_K &= (1 + (\widehat{\boldsymbol{\gamma}_1(\tau_1) - \mathbf{z}}) \cdot \boldsymbol{\gamma}_1(\tau_1)/c_0) \\ &\quad - \mu (1 + (\widehat{\boldsymbol{\gamma}_2(\tau_2) - \mathbf{z}}) \cdot \boldsymbol{\gamma}_2(\tau_2)/c_0), \quad (28)\end{aligned}$$

and

$$\begin{aligned}\partial_\mu \Phi_K &= -\omega_0 t (1 + (\widehat{\boldsymbol{\gamma}_2(\tau_2) - \mathbf{z}}) \cdot \boldsymbol{\gamma}_2(\tau_2)/c_0) \\ &\quad + \omega_0 t' (1 + (\widehat{\boldsymbol{\gamma}_2(\tau_2) - \mathbf{z}'}) \cdot \boldsymbol{\gamma}_2(\tau_2)/c_0). \quad (29)\end{aligned}$$

Then, the stationary points of the phase satisfy $\partial_{t,\mu}\Phi_K = 0$, implying that the stationary points are

$$\mu = \frac{(1 + (\widehat{\boldsymbol{\gamma}_1(\tau_1) - \mathbf{z}}) \cdot \boldsymbol{\gamma}_1(\tau_1)/c_0)}{(1 + (\widehat{\boldsymbol{\gamma}_2(\tau_2) - \mathbf{z}}) \cdot \boldsymbol{\gamma}_2(\tau_2)/c_0)} \quad (30)$$

and

$$t = t' \frac{(1 + (\widehat{\boldsymbol{\gamma}_2(\tau_2) - \mathbf{z}'}) \cdot \boldsymbol{\gamma}_2(\tau_2)/c_0)}{(1 + (\widehat{\boldsymbol{\gamma}_2(\tau_2) - \mathbf{z}}) \cdot \boldsymbol{\gamma}_2(\tau_2)/c_0)}. \quad (31)$$

Thus

$$\begin{aligned}K(\boldsymbol{z},\boldsymbol{z}') \approx &\int \exp\left(\frac{-\mathrm{i}\,\omega_0 t' \left[h(\boldsymbol{z},\boldsymbol{z}',\tau_1,\tau_2) - h(\mathbf{z}',\mathbf{z},\tau_1,\tau_2) \right]}{(1 + (\widehat{\boldsymbol{\gamma}_2(\tau_2) - \mathbf{z}}) \cdot \boldsymbol{\gamma}_2(\tau_2)/c_0)} \right) \\ &\times Q_{12}(\boldsymbol{z},t,\tau_1,\tau_2,\mu) A_{12}(\boldsymbol{z}',t',\tau_1,\tau_2,\mu) \\ &\times\ dt'\, d\tau_1\, d\tau_2 \quad (32)\end{aligned}$$

where μ and t should be understood as functions in $(\tau_1,\tau_2,\mathbf{z})$ and $(t',\tau_1,\tau_2,\mathbf{z},\mathbf{z}')$ defined by (30) and (31), respectively, and

$$\begin{aligned}h(\boldsymbol{z},\boldsymbol{z}',\tau_1,\tau_2) &= (1 + (\widehat{\boldsymbol{\gamma}_1(\tau_1) - \mathbf{z}'}) \cdot \boldsymbol{\gamma}_1(\tau_1)/c_0) \\ &\quad \times (1 + (\widehat{\boldsymbol{\gamma}_2(\tau_2) - \mathbf{z}}) \cdot \boldsymbol{\gamma}_2(\tau_2)/c_0). \quad (33)\end{aligned}$$

We expand $h(\boldsymbol{z},\boldsymbol{z}',\tau_1,\tau_2)$ and $h(\boldsymbol{z}',\boldsymbol{z},\tau_1,\tau_2)$ around $\boldsymbol{z}' = \boldsymbol{z}$, and use the approximation

$$\begin{aligned}&h(\boldsymbol{z},\boldsymbol{z}',\tau_1,\tau_2) - h(\boldsymbol{z}',\boldsymbol{z},\tau_1,\tau_2) \\ &\approx \left[\nabla_1 h(\boldsymbol{z},\boldsymbol{z},\tau_1,\tau_2) - \nabla_2 h(\boldsymbol{z},\boldsymbol{z},\tau_1,\tau_2) \right] \cdot (\boldsymbol{z}' - \boldsymbol{z}), \quad (34)\end{aligned}$$

where $\nabla_{1,2}$ denotes the gradient with respect to first and second variables, to rewrite $K(\boldsymbol{z},\boldsymbol{z}')$ as

$$\begin{aligned}K(\boldsymbol{z},\boldsymbol{z}') \approx \int &\exp^{-\mathrm{i}\boldsymbol{\xi}\cdot(\boldsymbol{z}'-\boldsymbol{z})} Q_{12}(\boldsymbol{z},t',\tau_1,\tau_2,\mu) \\ &\times A_{12}(\boldsymbol{z}',t',\tau_1,\tau_2,\mu)\, dt'\, d\tau_1\, d\tau_2, \quad (35)\end{aligned}$$

where

$$\begin{aligned}\boldsymbol{\xi} &= \boldsymbol{\xi}(\boldsymbol{z},t',\tau_1,\tau_2) \\ &= \frac{\omega_0 t' \left[\nabla_1 h(\boldsymbol{z},\boldsymbol{z},\tau_1,\tau_2) - \nabla_2 h(\boldsymbol{z},\boldsymbol{z},\tau_1,\tau_2) \right]}{(1 + (\widehat{\boldsymbol{\gamma}_2(\tau_2) - \mathbf{z}}) \cdot \boldsymbol{\gamma}_2(\tau_2)/c_0)}. \quad (36)\end{aligned}$$

Thus, changing variables from (t', τ_1, τ_2) to $\boldsymbol{\xi}$ we have

$$K(\boldsymbol{z}, \boldsymbol{z}') \approx \int \exp^{-\mathrm{i}\boldsymbol{\xi}\cdot(\boldsymbol{z}'-\boldsymbol{z})} Q_{12}(\boldsymbol{z}, \boldsymbol{\xi}) A_{12}(\boldsymbol{z}', \boldsymbol{\xi}) \eta(\boldsymbol{\xi})\, d\boldsymbol{\xi}, \tag{37}$$

where $\eta(\boldsymbol{\xi})$ is the Jacobian given by

$$\eta(\boldsymbol{\xi}) = \left| \frac{\partial \boldsymbol{\xi}}{\partial(t', \tau_1, \tau_2)} \right|^{-1}. \tag{38}$$

Thus, choosing Q_{12} as

$$Q_{12}(\boldsymbol{z}, \boldsymbol{\xi}) = \left[A_{12}(\boldsymbol{z}, \boldsymbol{\xi}) \eta(\boldsymbol{\xi}) \right]^{-1}, \tag{39}$$

the leading order term of the point spread function $K(\boldsymbol{z}, \boldsymbol{z}')$ becomes the Dirac delta function. With this choice of the weighting function, the resulting image formation algorithm recovers the visible edges of the scene radiance not only at the right location, but also at the right strength.

V. Conclusion

In this paper, we developed a novel correlation based weighted-backprojection type image formation method for passive SAR that uses transmitters of opportunity with fixed-frequency waveforms. The method is based on the scaled and windowed correlation of the received signals. Such correlation removes the transmitter related terms from the phase of the resulting wave propagation model allowing us to perform backpropagation to the right location on the ground without having the knowledge of the transmitter location. While the transmitter location is removed from the phase term, it remains in the amplitude term of the resulting operator. However, amplitude term only determines the strength, but not the location of the singularities. As such, it is less important than the phase term. To keep our discussion focused we assume that the location of the transmitter is known so as to determine the amplitude term (i.e., the geometric spreading factors) correctly without additional notation and derivation. However, this assumption can be avoided by treating the transmitted antenna beam pattern as a random quantity and assuming that *a priori* statistical information on the transmit antenna beam patterns are available. See our work in [7], [8]. To keep our discussion simple and focused, we also assume that there are two airborne receivers. However, this assumption is also not necessary. See [7], [8].

Windowed and scaled correlations of the received signal results in projection of the ground radiance onto the curves defined by the intersection of the constant Doppler cones with the ground topography. We next use microlocal analysis to recover ground radiance from its projections. The resulting image formation algorithm puts the visible edges of the scene radiance at the right location with right strength. Furthermore, the inversion is analytic. Therefore, the resulting algorithm can be made computationally efficient.

In the final version of our paper, we will present numerical simulation experiments to demonstrate the performance of our image formation algorithm.

Acknowledgments

B. Yazici's work is supported by the Air Force Office of Scientific Research[1] under the agreements FA9550-04-1-0223 and FA9550-07-1-0363.

References

[1] H. Griffiths and C. Baker, "Passive coherent location radar systems. part 1: Performance prediction," *IEE Proc.-Radar Sonar Navig.*, vol. 152, no. 3, June 2005.

[2] D. Poullin, "Passive detection using digital broadcasters (DAB, DVB) with COFDM modulation," *IEE Proc.-Radar Sonar Navig.*, vol. 152, no. 3, pp. 143–152, June 2005.

[3] R. Pollard, "The role of passive radar sensors for air traffic control."

[4] H. Griffiths and N. Long, "Television-based bistatic radar," *IEE Proc.-Radar Sonar Navig.*, vol. 133, no. 7, pp. 649–657, 1986.

[5] J. Homer, K. Kubik, B. Mojarrabi, I. Longstaff, E. Donskoi, and M. Cherniakov, "Passive bistatic radar sensing with leos based transmitters," in *Proceedings of IEEE International Geoscience and Remote Sensing Symposium*, 2002.

[6] M. Cherniakov, R. Saini, R. Zuo, and M. Antoniou, "Space surface bistatic sar with space-borne non-cooperative transmitters," in *Proceedings of European Radar Conference*, Oct. 2005, pp. 25–28.

[7] C. Yarman, B. Yazici, and M. Cheney, "Bistatic synthetic aperture hitchhiker imaging with non-cooperative sources of opportunity," in *Proceedings of SPIE Defense and Security Symposium*, April 2007, p. 65806.

[8] ——, "Bistatic synthetic aperture hitchhiker imaging," in *IEEE ICASSP*, April 2007, pp. I–537 – I–540.

[9] B. Borden and M. Cheney, "Synthetic-aperture imaging from high-doppler-resolution measurements," *Inverse Problems*, vol. 21, pp. 1–11, 2005.

[10] V. Koch and R. Westphal, "New approach to a multistatic passive radar sensor for air/space defense," *IEEE Aerospace and Electronic Systems Magazine*, vol. 10, pp. 24–32, Nov. 1995.

[11] M. Cherniakov, K. Kubik, and D. Nezlin, "Bistatic synthetic aperture radar with non-cooperative leos based transmitter," in *Proceedings of IEEE International Geoscience and Remote Sensing Symposium*, vol. 2, July 2000, pp. 861–862.

[1]Consequently the U.S. Government is authorized to reproduce and distribute reprints for Governmental purposes notwithstanding any copyright notation thereon. The views and conclusions contained herein are those of the authors and should not be interpreted as necessarily representing the official policies or endorsements, either expressed or implied, of the Air Force Research Laboratory or the U.S. Government.

[12] ——, "Radar sensors based on communication low earth orbiting satellites microwave emission," in *Proceedings of IEEE International Geoscience and Remote Sensing Symposium*, vol. 3, July 2000, pp. 1007–1008.
[13] P. Howland, D. Maksimiuk, and G. Reitsma, "Fm radio based bistatic radar."
[14] C. Baker, H. Griffiths, and I. Papoutsis, "Passive coherent location radar systems. part 2: Waveform properties," *IEE Proc.-Radar Sonar Navig.*, vol. 152, no. 3, pp. 160–168, June 2005.
[15] D. Tan, H. Sun, Y. Lu, M. Lesturgie, and H. Chan, "Passive radar using global system for mobile communication signal: theory, implementation and measurements," *IEE Proc.-Radar Sonar Navig.*, vol. 152, no. 3, pp. 116–123, June 2005.
[16] X. He, M. Cherniakov, and T. Zeng, "Signal detectability in ssbsar with gnss non-cooperative transmitter," *IEE Proc.-Radar Sonar Navig.*, vol. 152, no. 3, pp. 124–132, June 2005.
[17] C. Nolan and M. Cheney, "Synthetic aperture inversion for arbitrary flight paths and non-flat topography," *IEEE Transactions on Image Processing*, vol. 12, pp. 1035–1043, 2003.
[18] H. Barrett and K. Myers, *Foundations of image science*. Hoboken, NJ: Wiley-Interscience, 2004.
[19] F. Treves, *Introduction to Pseudodifferential and Fourier Integral Operators, volumes I and II*. New York: Plenum Press, 1980.
[20] G. Salmon, *Treatise on Conic Sections*, 6th ed. American Mathematical Society, 2006.
[21] N. Willis, *Bistatic Radar*. Norwood, MA: Artech House, 1991.

APPENDIX I
INTERSECTION OF A CONSTANT-DOPPLER CONE WITH A FLAT SURFACE

Let $\boldsymbol{\gamma}(t)$ be a receiver flight trajectory with velocity $\dot{\boldsymbol{\gamma}}(t) = \mathbf{v}(t)$. The constant-Doppler cone is defined by (see (21))

$$(\boldsymbol{\gamma}(t) - \mathbf{z}) \cdot \mathbf{v}(t) = v\,|\boldsymbol{\gamma}(t) - \mathbf{z}|. \tag{40}$$

Assuming we have a flat earth surface, we write $\mathbf{z} = [z_1, z_2, 0]$. For fixed t, we rewrite (40) as

$$k - [v_1 z_1 + v_2 z_2] = v\sqrt{(\gamma_1 - z_1)^2 + (\gamma_2 - z_2)^2 + \gamma_3^2}, \tag{41}$$

where $k = \boldsymbol{\gamma}(t) \cdot \mathbf{v}(t)$, $\mathbf{v}(t) = [v_1, v_2, v_3]$ and $\boldsymbol{\gamma}(t) = [\gamma_1, \gamma_2, \gamma_3]$. We square both sides of (41) and obtain

$$az_1^2 + 2bz_1z_2 + cz_2^2 + 2dz_1 + 2fz_2 + g = 0, \tag{42}$$

where

$$\begin{aligned} a &= (v_1^2 - v^2) \\ b &= v_1 v_2 \\ c &= (v_2^2 - v^2) \\ d &= v^2\gamma_1 - kv_1 \\ f &= v^2\gamma_2 - kv_2 \\ g &= k^2 - v^2(\gamma_1^2 + \gamma_2^2 + \gamma_3^3). \end{aligned}$$

(42) defines a conic section [20] and defines an ellipse, parabola or hyperbola if $\Delta = b^2 - ac$ is smaller than, equal to or larger than zero. By (21), $v = |\mathbf{v}|\cos\theta$, where θ is the angle between $\widehat{(\boldsymbol{\gamma}(t) - \mathbf{z})}$ and $\mathbf{v}$. Thus

$$\begin{aligned} \Delta &= v_1^2 v_2^2 - (v_1^2 - v^2)(v_2^2 - v^2) \\ &= v^2(v_1^2 + v_2^2 - v^2) \\ &= v^2(|\mathbf{v}|^2(1 - \cos^2\theta) - v_3^2) \end{aligned} \tag{43}$$

For receiver trajectories at a constant altitude $v_3 = 0$, $\Delta > 0$ hence the intersection of constant-Doppler cone with flat earth surface gives a hyperbola, which is also known as iso-doppler contour [21].

APPENDIX II
CONSTANT-DOPPLER CONES AND $\mathcal{F}$

Let $\boldsymbol{\gamma}_{1,2}$ be two flight trajectories. The constant-Doppler cones with respect to $\boldsymbol{\gamma}_{1,2}$ are given by

$$\widehat{(\boldsymbol{\gamma}_1(\tau_1) - \mathbf{z})} \cdot \dot{\boldsymbol{\gamma}}_1(\tau_1) = v_1(\tau_1, \mathbf{z}) \tag{44}$$

and

$$\widehat{(\boldsymbol{\gamma}_2(\tau_2) - \mathbf{z})} \cdot \dot{\boldsymbol{\gamma}}_2(\tau_2) = v_2(\tau_2, \mathbf{z}), \tag{45}$$

for some $v_{1,2} \in \mathbb{R}$. Substituting (44) and (45) in (20), we have

$$v_1(\tau_1, \mathbf{z}) - \mu v_2(\tau_2, \mathbf{z}) = (\mu - 1)c_0. \tag{46}$$

Thus, for fixed $\tau_{1,2}$ and $\mathbf{z}$, $\mathcal{F}$ obtains its leading order terms when

$$\mu(\tau_1, \tau_2, \mathbf{z}) = \frac{v_1(\tau_1, \mathbf{z}) + c_0}{v_2(\tau_2, \mathbf{z}) + c_0}, \tag{47}$$

Alternatively, for fixed τ_1, μ and $\mathbf{z}$, $\mathcal{F}$ obtains its leading order term for τ_2, that satisfies

$$v_2(\tau_2, \mathbf{z}) = \frac{v_1(\tau_1, \mathbf{z}) - (\mu - 1)c_0}{\mu}. \tag{48}$$

Here τ_2 should be regarded as a function of $(\tau_1, \mu, \mathbf{z})$. Consequently, we can develop a similar argument for τ_1 by fixing τ_2, μ and $\mathbf{z}$.